Quaternary Science Reviews 48 (2012) 99–112

Contents lists available at SciVerse ScienceDirect

Quaternary Science Reviews

journal homepage: www.elsevier.com/locate/quascirev

Regional imprints of millennial variability during the MIS 3 period around Antarctica

D. Buiron [a], B. Stenni [b,*], J. Chappellaz [a], A. Landais [c], M. Baumgartner [d,g], M. Bonazza [b], E. Capron [c,1], M. Frezzotti [e], M. Kageyama [c], B. Lemieux-Dudon [f], V. Masson-Delmotte [c], F. Parrenin [a], A. Schilt [d,g], E. Selmo [h], M. Severi [i], D. Swingedouw [c], R. Udisti [i]

[a] Laboratoire de Glaciologie et Géophysique de l'Environnement (LGGE), CNRS and University of Grenoble I, 38400 Saint Martin d'Hères, France
[b] Department of Mathematics and Geosciences, University of Trieste, 34127 Trieste, Italy
[c] Laboratoire des Sciences du Climat et de l'Environnement, IPSL/CEA-CNRS-UVSQ, UMR 8212, CEA Saclay, L'Orme des Merisiers, Bât. 701, 91191 Gif-sur-Yvette Cedex, France
[d] Climate and Environmental Physics, Physics Institute, University of Bern, Sidlerstrasse 5, CH-3012 Bern, Switzerland
[e] ENEA, CR Casaccia, 00123 Roma, Italy
[f] INRIA – Laboratoire Jean Kuntzmann, B.P. 53, 38000 Grenoble, France
[g] Oeschger Centre for Climate Change Research, University of Bern, CH-3012 Bern, Switzerland
[h] Department of Earth Sciences, University of Parma, 43100 Parma, Italy
[i] Department of Chemistry, University of Firenze, 50019 Sesto Fiorentino, Italy

ARTICLE INFO

Article history:
Received 16 November 2011
Received in revised form
29 May 2012
Accepted 31 May 2012
Available online

Keywords:
Paleoclimate
Millennial-scale variability
Glacial period
Ice cores
Talos Dome
Global coupled model simulations

ABSTRACT

The climate of the last glacial Marine Isotopic Stage 3 (MIS3) period is characterized by strong millennial-scale variability with a succession of Dansgaard–Oeschger events first identified in Greenland ice cores and associated with variations of the Atlantic Meridional Overturning Circulation (AMOC). These abrupt events have a smooth and lagged counterpart in water stable isotopes from Antarctic ice cores. In this study we aim at depicting and understanding the circum-Antarctic expression of this millennial-scale variability. To illustrate the mechanisms potentially at work in the response of the southern high latitudes to an abrupt decrease of the AMOC, we first present results from experiments performed with the IPSL-CM4 atmosphere-ocean coupled model under glacial boundary conditions. When the AMOC is perturbed by imposing an additional freshwater flux in the North Atlantic, our model produces the classical bipolar seesaw mechanism generally invoked to explain the warming of the Southern Ocean/Antarctic region. However, this mechanism can be locally offset by faster atmospheric teleconnections originating from the tropics, even though the precise location of this fast response is not coherent among different climate models. Our model results are confronted with a synthesis of Antarctic records of ice core stable isotope and sea-salt sodium, including new data obtained on the TALDICE ice core. The IPSL-CM4 produces a dipole-like pattern around Antarctica, with warming in the Atlantic/Indian sectors contrasting with an unexpected cooling in the East-Pacific sector. The latter signal is not detected in our data synthesis. Both ice core data and simulations are consistent in depicting a more rapid response of the Atlantic sector compared to the Indian sector. This feature can be explained by the gradual impact of ocean transport on which faster atmospheric teleconnections are superimposed. Detailed investigations of the sequence of events between different proxies are conducted in three ice cores. Earlier shifts in deuterium excess and significant changes in sea-salt sodium fluxes in the most coastal sites (TALDICE and EDML) compared to EDC suggest reorganizations in local moisture sources, possibly linked with sea-ice cover. This study demonstrates the added value of circum-Antarctic ice core records to characterize the patterns and mechanisms of glacial climate variability.

1. Introduction

During the last glacial Marine Isotopic Stage 3 period (MIS3), global climate underwent strong millennial-scale fluctuations. Paleoclimatic archives reveal that the Northern Hemisphere experienced repeated abrupt warming phases known as

* Corresponding author.
E-mail address: stenni@units.it (B. Stenni).
[1] Now at British Antarctic Survey, High Cross, Madingley Road, CB3 0ET Cambridge, United Kingdom.

0277-3791/$ – see front matter © 2012 Elsevier Ltd. All rights reserved.
http://dx.doi.org/10.1016/j.quascirev.2012.05.023

Dansgaard–Oeschger (DO) events, characterized by shifts of up to 16 °C between stadials (cold phases) and interstadials (warm phases) occurring within a few decades in Greenland (Dansgaard et al., 1993; Severinghaus et al., 1998; Lang et al., 1999; Landais et al., 2004). Several of the DO events were preceded by Heinrich events, massive iceberg discharges from the Northern Hemisphere ice sheets (Heinrich, 1988). Large releases of freshwater into the Atlantic Ocean are probably associated to a weakening of the Atlantic Meridional Overturning Circulation (AMOC) (Vidal et al., 1997; Elliot et al., 2002; McManus et al., 2004) although the question of the initial triggering mechanism for this freshwater flux, and timing compared to the AMOC collapse, remains an open question (cf. Alvarez-Solas and Ramstein, 2011). Ocean models show that such a decrease in the AMOC intensity affects the bipolar heat distribution, leading to a cooling of the North Atlantic region and a warming of the South Atlantic (Crowley, 1992; Stocker, 1998). The strong Southern Ocean (SO) circumpolar current is then expected to propagate this anomaly around the Antarctic continent. Precise synchronisation of Antarctic and Greenland ice core records (Blunier et al., 1998; Blunier and Brook, 2001; EPICA Community Members, 2006; Capron et al., 2010) has allowed characterizing the phase relationships of north-south climate variability. During stadial phases in Greenland, a gradual warming occurs in Antarctica (~2 °C/1000 years). This warming is then interrupted after a few thousands of years and Antarctica starts to cool gradually (~2 °C/1000 years), concomitant with the onset of an abrupt warming event in Greenland. A systematic one-to-one correspondence has been established between stadial–interstadial transitions in Greenland, and Antarctic Isotope Maximum (AIM) events during the last glacial period (Blunier et al., 1998; Blunier and Brook, 2001; EPICA Community Members, 2006; Capron et al., 2010). Such out-of-phase relationship between the two poles can be explained by the thermal bipolar seesaw concept (Broecker, 1998) where the SO acts as a heat reservoir affected by the AMOC strength (Stocker and Johnsen, 2003; Barker et al., 2009).

Because of the central role of the Atlantic Ocean in the bipolar seesaw mechanism, one may expect strong regional differences for the expression of the AIM events in the different sectors of the SO around Antarctica. Stenni et al. (2010) have compared the shapes of the AIM events observed between two different ice cores in Antarctica (described in Table 1): the EPICA (European Project for Ice Coring in Antarctica) Dome C (EDC) ice core drilled in the Indian sector is characterised by triangular AIM events (EPICA Community Members, 2004; Jouzel et al., 2007), while the EPICA Dronning Maud Land (EDML) ice core drilled in the Atlantic sector shows more squared AIM event shapes (EPICA Community Members, 2006). These data suggest, in response to AMOC weakening, a faster response in the Atlantic than in the Indian Ocean sector. At a broader scale, there is also little information available on changes in SO sea surface temperatures (SST). Lamy et al. (2004) and Kaiser et al. (2005) suggest that latitudinal shifts of the Antarctic circumpolar current/southern westerly were similar for all locations of the SO, implying that changes in SST/atmospheric circulation/surface ocean circulation are zonally homogeneous and simultaneous for the SO. This contrasts with the findings from Antarctica arising a question about the possibilities of zonal asymmetries in the abrupt climate changes in the southern high latitudes, and which processes could explain them.

On the modelling side several simulations have already been carried out with coupled ocean-atmosphere General Circulation Models (hereafter, noted GCM) to identify the mechanisms responsible for the climatic system behaviour observed during millennial-scale abrupt events. These were first performed under modern boundary conditions (e.g., Manabe and Stouffer, 1988) but the most recent experiments were performed under Last Glacial Maximum (Kageyama et al., 2009; Otto-Bliesner and Brady, 2010) or even Marine Isotopic Stage 3 (Merkel et al., 2010) boundary conditions. DO or Heinrich events are mimicked by prescribing an abrupt freshwater release in the North Atlantic region (Stouffer et al., 2006; Timmermann et al., 2010). All these models have confirmed the robustness of the bipolar seesaw signature of the climate response to AMOC weakening: the South Atlantic Ocean warms while a cooling is observed in the North Atlantic region and this is accompanied by a southern shift of the Intertropical Convergence Zone (ITCZ) (Dahl et al., 2005; Broccoli et al., 2006; Krebs and Timmermann, 2007; Swingedouw et al., 2009). While the South Atlantic systematically warms in response to a freshwater discharge applied in the North Atlantic, there are regional differences in the simulated SO response (Timmermann et al., 2010, in addition to the reviews of Clement and Peterson, 2008 and Kageyama et al., 2010). Some models simulate a quasi-uniform warming (e.g. Otto-Bliesner and Brady, 2010) while others show contrasted patterns with a West Pacific cooling associate with the Southern Indian Ocean sector warming. Timmermann et al. (2010) attribute such dipole-like surface air temperature to an intensification of the negative phase of the atmospheric Pacific South America mode (PSA). Anomalies in the meridional heat advection are simulated to produce an anomalous cyclonic circulation in the Amundsen-Bellingshausen Sea. Simulated regional circum-Antarctic temperature anomalies coincide with regional sea ice extent changes, amplified by sea ice albedo feedbacks. Analyzing atmosphere-only experiments in which SST anomalies from the

Table 1
Description of the different drilling sites.

Site	Latitude (south)	Longitude	Elevation (m)	Distance to coast (km)	Current surface temperature (°C)	Current accumulation rate (mm w.eq./yr)	Geographical sector according to this paper division	Isotopic data resolution between 20 and 50 ky BP (yr)	References
TALDICE	72°48′	159°06E	2318	250	−41	80.5	Indian	88.9	(Frezzotti et al., 2004) (Stenni et al., 2011)
EDC	75°10′	123°35E	3240	870	−54.5	26.9	Indian	48.3	(EPICA Community Members, 2004) (Jouzel et al., 2007)
Vostok	78°28′	106°48E	3490	1260	−55.5	21.8	Indian	82.1	(Petit et al., 1999)
Taylor Dome	77°48′	158°43E	2365	120	−43	47.4–66.3	Ross Sea	101.5	(Steig et al., 1998)
Siple Dome	81°66′	148.8W	621	470	−24.5	106.1	East-Pacific	91.3	(Brook et al., 2005)
Byrd	80°01′	119°31W	1530	620	−28	94.7–113.6	East-Pacific	100.1	(Blunier and Brook, 2001)
EDML	75°00′	0°01E	2892	529	−43.2	60.6	Atlantic	100.0	(EPICA Community Members, 2006)
Dome F	77°19′	39°42E	3810	1000	−57.3	25–30	Atlantic	250.0	(Watanabe et al., 2003)

perturbed coupled simulation are prescribed only on restricted regions, Timmermann et al. (2010) relate this anomalous behaviour of the South Pacific to SST anomalies from the Tropical Pacific. Ding et al. (2011) explain the link between the central equatorial Pacific and the Pacific sector of East Antarctica climate through atmospheric Rossby waves propagating from the tropics to Antarctica. Atmospheric teleconnections have therefore the potential to cause zonal asymmetries in the circum-Antarctic response to AMOC changes.

Here, we aim at better documenting the regional patterns of temperature evolution around Antarctica during AIM events. For this purpose, we compare a synthesis of existing and new high-resolution Antarctic ice core data covering the last 50 ky (thousands of years) and climatic simulations. In Section 2 we analyze the circum-Antarctic response to a freshwater perturbation applied in the North Atlantic simulated by the global coupled climate model IPSL-CM4. Section 3 presents the ice core proxy data used to document past regional changes in temperature, moisture origin and sea-ice extent, and the consistency of the available chronologies. Section 4 presents new detailed measurements ($\delta^{18}O$, d-excess, sea salt sodium, $ssNa^{+}$) performed on the Talos Dome (TALDICE) ice core, drilled on the edge of the East Antarctic plateau (Frezzotti et al., 2004), and a detailed comparison with other Antarctic ice cores. This database yields a comprehensive picture of the AIM event expression in different sectors of Antarctica. Section 5 discusses these results and compares them to the model results presented in this introduction and Section 2.

2. Climatic simulations

We analyze two simulations performed with the coupled atmosphere-ocean climate model IPSL-CM4 (Kageyama et al., 2009; Marti et al., 2010). Both simulations use Last Glacial Maximum (LGM) climate boundary conditions (PMIP2 protocol, Braconnot et al., 2007): the ICE-5G ice-sheet reconstruction (Peltier, 2004), and greenhouse gases atmospheric mixing ratios of 185 ppm, 350 ppb and 200 ppb for CO_2, CH_4 and N_2O, respectively (Flückiger et al., 1999; Dällenbach et al., 2000; Monnin et al., 2001) are prescribed, as well as 21 ky orbital parameters (Berger, 1978). The vegetation cover remains similar to modern conditions over ice-free areas but river pathways have been adapted for LGM conditions (Alkama et al., 2007). The reference simulation (LGM-ref) has a stable AMOC at around 15 Sv. To simulate a rapid cooling event in the North Atlantic through a collapse of the AMOC, we have imposed, starting from the end of year 149 of the reference run, an additional 0.1 Sv freshwater flux in the North Atlantic and the Arctic (Kageyama et al., 2009). This 419-year long freshwater hosing simulation (LGM-fw) is characterized by a very large reduction in the AMOC strength (Fig. 1a), and provides an idealized scenario of what may have happened at the onset of a Heinrich event such as H2 or H1, which occurred close to the LGM.

The Surface Air Temperature (SAT, taken at 2 m above the surface) anomaly induced by the AMOC shutdown is shown in Fig. 1b. The North Atlantic region gets cooler when the AMOC is reduced, whereas the South Atlantic warms, expressing a bipolar seesaw. The NH (Northern Hemisphere) cools locally by 9 °C whereas the SH (Southern Hemisphere) warming is more muted (up +3 °C). This is consistent with ice core temperature estimates during AIM events (Stenni et al., 2010) (see also Section 5.1). The most surprising feature concerns the zonal asymmetries in the temperature response in the SO and their Antarctic signatures. Strong positive anomalies are simulated in the South Atlantic and Indian Oceans, whereas the Southeast Pacific sector undergoes a slight cooling, leading to a dipole pattern in the southern thermal response.

As summarized in Section 1, the mechanism at the origin of such regional disparities could originate from a fast atmospheric teleconnection from the tropics to the southern Pacific. In our simulation (Fig. 2b), the freshwater flux leads to a cooling in the northern tropical Atlantic and a warming in the southern tropical Atlantic. As described in Kageyama et al. (2009), the southward ITCZ shift is strongest in the Atlantic Ocean and surrounding continents. This disturbance in the tropical large-scale circulation is responsible for an atmospheric stationary wave propagating southeastward over the tropical Pacific and then southward over the southeast Pacific Ocean. Fig. 2b highlights the centres of action of this wave in Austral winter (June, July, August) 200 hPa stream function anomaly, with a positive centre at 100°W and 20°S, a negative centre at 120°W and 40°S and a broad positive centre at around 60°S in the southeast Pacific. These centres correspond to underlying surface temperature anomalies, with a slight southward shift of the upper circulation anomalies compared to the surface temperature ones. A similar wave is developing above the South Atlantic Ocean. Sensitivity tests to Atlantic or Pacific SST anomalies,

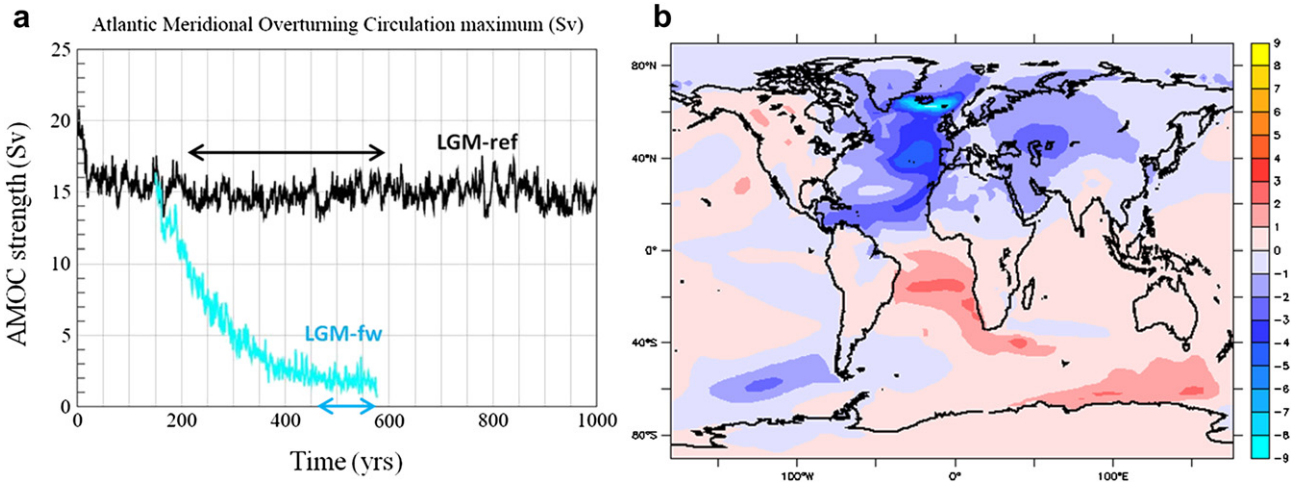

Fig. 1. a: Time evolution (in years) of the AMOC strength in simulations LGM-ref (black) and LGM-fw (cyan), expressed in Sv (1 Sv = 106 m^3/s). In LGM-fw, there is a prescribed release of 0.1 Sv of freshwater in the North Atlantic and Arctic oceans. Arrows underline the periods used for the calculation of the final mean surface atmospheric temperature (SAT) anomaly represented on the right panel of this figure. b: Mean annual SAT anomaly (in °C) between LGM-ref (averages values between years 200 and 600) and the last 100 yr of LGM-fw. (For interpretation of the references to colour in this figure legend, the reader is referred to the web version of this article.)

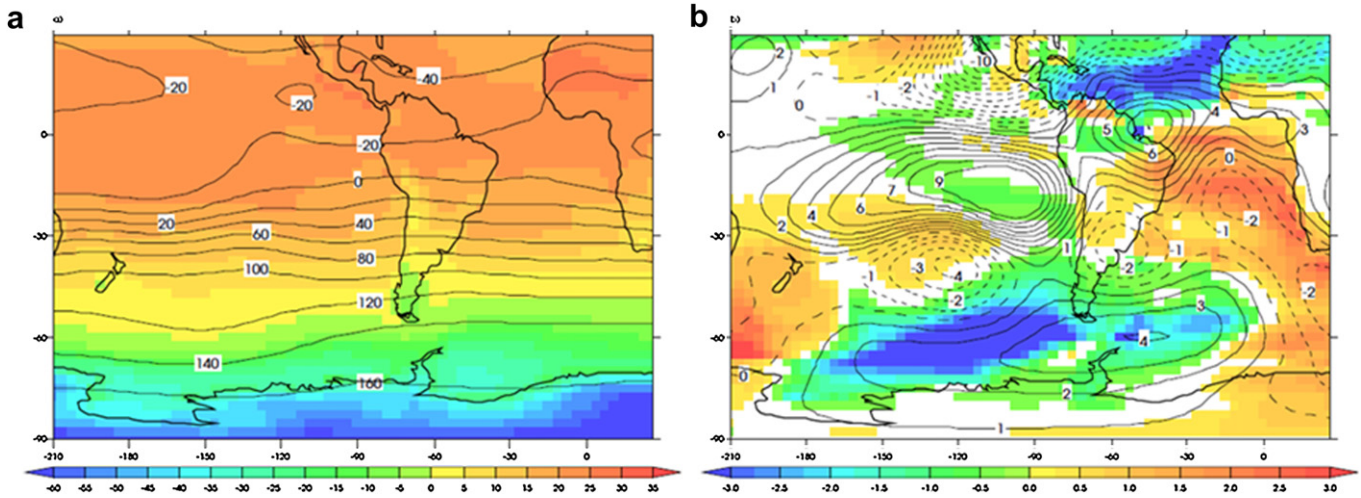

Fig. 2. Teleconnection from the tropical Atlantic to the Southeast Pacific and Antarctica. Results from the Atmosphere-only GCM, using different surface ocean forcing. All fields are shown for June-July-August. a: Reference run LGM-refatm, using surface ocean conditions from LGM-ref: SAT (°C, shading) and 200 hPa stream function (106 m^2/s, contours). b: Anomalies in SAT (°C, shading) and stream function (106 m^2/s, contours, dashed for zero line, dotted for negative values) for the FW-global SST experiment.

using atmosphere-only simulations are reported in the Appendix (Section III). This suggests that tropical Atlantic SST changes alone can generate a stationary wave reaching the southeast Pacific.

In order to better quantify the simulated spatial and temporal features associated with the SO and Antarctic response to the AMOC weakening, we divided this region into four sectors: the Atlantic, Indian, West-Pacific/Ross Sea, and East-Pacific sectors (Fig. 3). Fig. 4 displays the mean SAT and sea-ice evolutions in the course of the LGM-fw simulation for each sector, and averaged between 40 and 80°S. The differences observed between the mean SAT of each sector reflects at least partly the difference of the land-sea surface ratio between each sector in the 40-80°S latitude range. To complement this study, we also calculated the SAT evolution in each sector between 40 and 60°S and between 60 and 80°S separately (not shown in this paper). Even if the mean SAT of each sector varies considering those different latitude ranges, the SAT evolutions obtained show similar patterns as the ones calculated for latitudes between 40 and 80°S. As our main interest lies in SAT variations and not in SAT absolute value, we finally chose to show only the 40-80°S SAT evolution in Fig. 4.

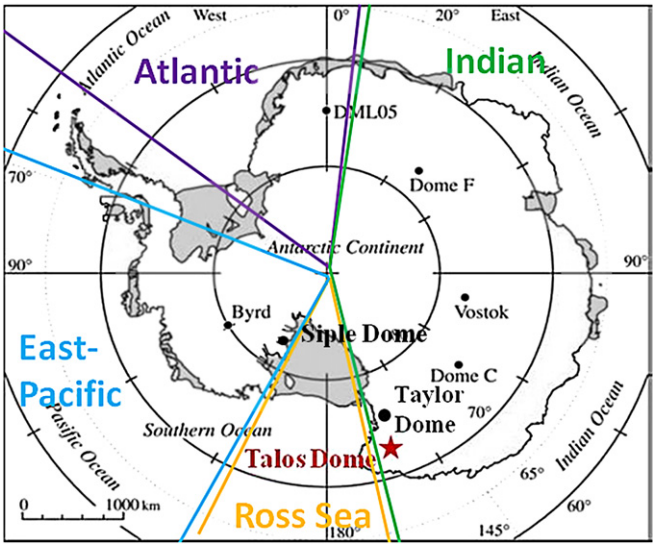

Fig. 3. Map showing the division of the Southern Ocean and Antarctica into four sectors: an Indian sector located between 15°E and 160°E and between 40°S and 80°S, an Atlantic sector located between 15°E and 50°W and between 40°S and 80°S, a West-Pacific/Ross Sea sector located between 160°E and 150°W and between 40°S and 80°S, and an East-Pacific sector located between 150°W and 75°W and between 40°S and 80°S.

This comparison highlights specific features, amplitudes, and rates of temperature changes through the different ocean sectors, summarized in Table 2. A strong consistency is depicted between simulated SAT and sea-ice extent. The following differences appear between the simulated climatic responses in the different sectors:

- The fastest temperature changes (+1 °C within 50 years) are simulated in the Atlantic sector. These large temperature variations mainly affect the oceanic sector between about 78 and 65°S.
- A smaller linear increasing trend is detected in the Indian sector (+1 °C over >300 years). Even if stronger over ocean than land areas, these large temperature variations have a wide impact: they concern both the oceanic and Antarctic continent down to latitude of about 85°S.
- In contrast to the Atlantic and Indian sectors, a cooling trend (−0.7 °C in >100 years) associated with a regional sea-ice expansion is depicted in the East-Pacific. This SAT anomaly mainly affects the oceanic sector between about 70 and 40°S.
- No centennial trend is detected in the Western Pacific and Ross Sea sector, where temperature variability is the weakest and occurs on decadal time scales. SAT variations only concern oceanic areas with a cooling trend down to 70°S, and a warm anomaly at northern latitudes (see Fig. 1b).

In summary, the LGM-fw simulation shows a persistent zonal dipole in temperature between the East-Pacific and Indian sectors. The freshwater hosing of around 0.1 Sv in the North Atlantic and Arctic Oceans produces sharp changes in the early part of the simulation in the Atlantic and East-Pacific sectors which are not counteracted by a warming due to the bipolar seesaw and advected by the SO circulation. This behaviour was also shown by several climate models under both modern and LGM boundary conditions (cf. the multi-model study of Timmermann et al., 2010) while a few other models (e.g. Merkel et al., 2010) depict a SO temperature response, which is nearly zonally symmetric. For models, which do show a zonally asymmetric response of the SO to a freshwater

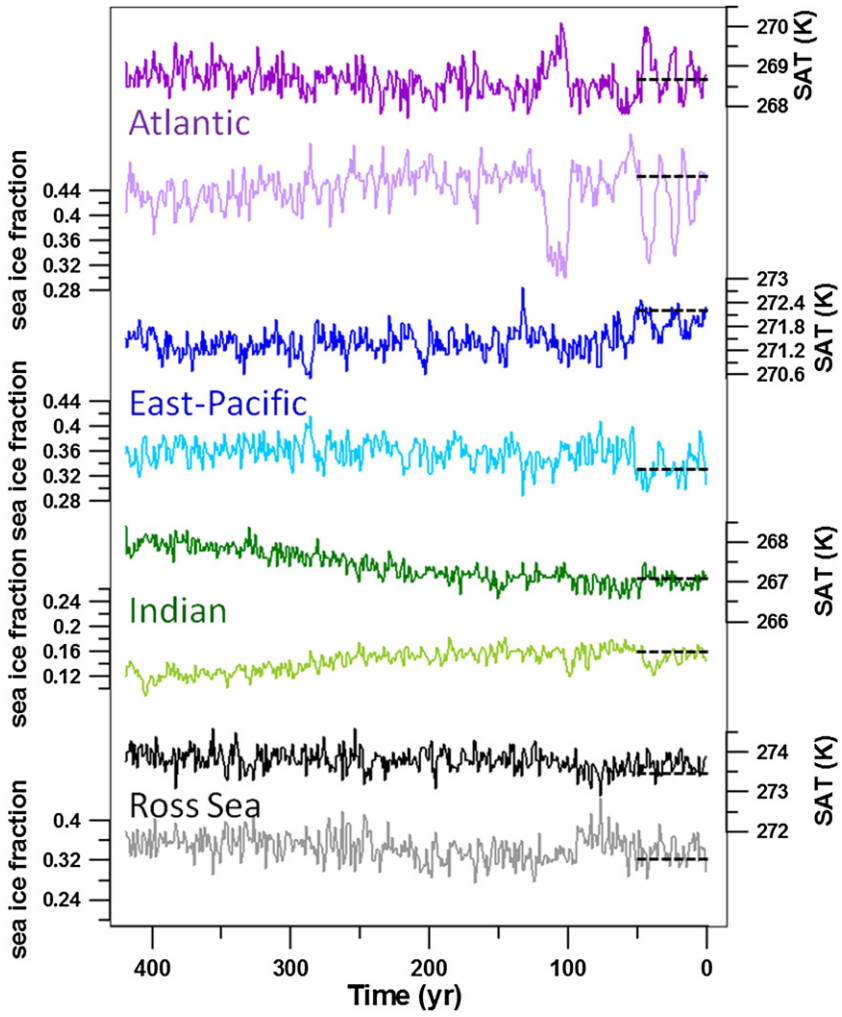

Fig. 4. Climate anomalies simulated by the IPSL-CM4 model in the southern area. LGM-ref-LGM-fw Surface Air Temperature, SAT (in K) and sea-ice fraction evolutions in the Atlantic (purple), East-Pacific (blue), Indian (Green) and West-Pacific/Ross Sea (black) sectors during the LGM-fw simulation. Dashed lines represent the initial values calculated as the average of the first ten years for each signal. (For interpretation of the references to colour in this figure legend, the reader is referred to the web version of this article.)

perturbation applied in the North Atlantic, the pattern of this response is not consistent from model to model. For instance, for LGM boundary conditions, the CCSM3 model response over the SO, as depicted in Otto-Bliesner and Brady (2010), is weaker (and even slightly negative) in the Atlantic sector of the SO. At this point, we conclude that the latest results from atmosphere-ocean climate models show the possibility of a fast response of the SO surface to perturbations in the AMOC forced by a freshwater flux imposed in the North Atlantic, stemming from atmospheric teleconnections from the tropics. This fast atmospheric response can weaken, or in some cases counteract, the slower bipolar thermal response of the ocean. The precise pattern of the zonal asymmetry does not appear

Table 2
Left part: amplitude and warming duration of AIM evens 8 and 12 in the different ice cores: the amplitude has been determined through data re-sampled on a 100 year time step. For TALDICE, EDML, and EDC sites calculations, please refer to the Appendix and to Section 4.1 of this paper. For other ice cores, the duration has been visually defined based on their own age scales. Right part: amplitude of the SAT variation simulated by the model during the LGM-fw simulation, and time requests to reach this total anomaly (from the lowest to the highest SAT value taken on 30 years averaged data).

		Ice core data				Model results		
Ice core drilling site	Geographical sector according to this paper division	AIM 8 isotopic amplitude (‰)	AIM 12 isotopic amplitude (‰)	AIM 8 warming duration (yr)	AIM 12 warming duration (yr)	Amplitude of temperature change (°C)	Linear correlation coefficient for temperature data	Duration for the total temperature change (yr)
TALDICE	Indian	2.2	1.3	1650	1800	+1.23	0.54	328
EDC		2.7	3.2	1600	1600			
Vostok		2.0	2.7	1500	2400			
Taylor Dome	Ross Sea	3.3	4.3	1850	2000	+0.74	–	33
Siple Dome	East-Pacific	4.5	4.0	1000	2300	−0.71	0.024	118
Byrd		2.5	3.0	1800	2700			
EDML	Atlantic	2.2	1.9	850	970	+1.08	–	51
Dome F		1.3	1.3	750	1700			

to be consistent from model to model and is probably sensitive to the details of the scenario chosen to perform the freshwater hosing experiment. This sensitivity is confirmed by the systematic study of the response of the LOVECLIM model to an ensemble of freshwater hosing scenarios (Roche et al., 2010). Improving the spatio-temporal documentation of rapid climate changes at southern high latitudes is expected to provide an important test of the models and the scenarios used to mimic Heinrich events or stadials.

3. Material and methods

We use published and new Antarctic ice cores records to confront our modelling results with paleoclimatic evidence. In order to retrieve information on local temperature variations and on the evolution of the sea-ice extent, assumed to play an important role in the regional variability, we investigate measurements of water isotopes ($\delta^{18}O$) (a proxy of Antarctic temperature), deuterium excess ($d = \delta D - 8 \times \delta^{18}O$) (a proxy of moisture source evaporation conditions), and sea-salt sodium flux ($ssNa^{+}$) (suggested to be related to sea-ice extent).

3.1. Drilling sites

Our investigation of regional changes relies on 8 different ice cores (Fig. 3), whose characteristics are summarized in Table 1.

In particular, we present new measurements performed on the most recent ice core, TALDICE, drilled during the field seasons 2004–2008. The drilling of TALDICE reached a depth of 1620 m at a site located on the eastern edge of the East-Antarctic plateau in the Victoria Land, at roughly equal distance (~300 km) from the Southern Indian Ocean and the Ross Sea. As for current surface climatic conditions, the annual mean accumulation rate is 8.05 cm w.eq./yr (water equivalent per year) (Stenni et al., 2002; Frezzotti et al., 2007) and the annual mean air temperature is of −41 °C. Backtrajectory analyses show that TALDICE receives air masses arriving from the Indian Ocean (50%) and partially from the Pacific/Ross Sea sector (30%), the last 20% arriving from the Antarctic plateau (Sodemann and Stohl, 2009; Scarchilli et al., 2011; Masson-Delmotte et al., 2011). During glacial times and most of the deglaciation, the presence of the Ross Ice Sheet extending up to the continental margin should have reduced the precipitations coming from the Ross Sea area. The new measurements cover the MIS3 time period and complement the first dataset published by Stenni et al. (2011).

3.2. Water stable isotope data

The water stable isotope composition ($\delta^{18}O$ and δD) of Antarctic ice cores is an integrated tracer of the water cycle, mostly controlled by the condensation temperature. Along its transport from oceanic sources to ice core sites, atmospheric moisture is exposed to multiple fractionation processes at each phase change, causing a progressive distillation and loss of heavy isotopes. Despite the complexity of the different processes involved, the isotopic composition of Antarctic surface snow is linearly linked to the local surface air temperature (Lorius et al., 1979; Masson-Delmotte et al., 2008), with a spatial slope of 0.8‰/°C. This spatial relationship has been used for decades to estimate past temperatures using water stable isotope measurements from Antarctic ice cores. However, uncertainties exist in the stability of the isotope-temperature relationship through time, as it is sensitive to variations of the oceanic evaporative regions (Stenni et al., 2010) and of precipitation intermittency (Krinner and Werner, 2003). Temporal $\delta^{18}O$ – temperature slopes based on seasonal or interannual measurements in several Antarctic stations (Van Ommen and Morgan, 1997; Oerter et al., 2004) are associated with a value almost twice smaller (0.4‰/°C) than the spatial slope. While Sime et al. (2009) suggest a small isotope-temperature slope for warmer than present-day climates, Jouzel et al. (2003) suggest that the spatial relationship is a good approximation to reconstruct past glacial temperature with 20–30% uncertainty. Moreover, Stenni et al. (2010) have shown limited impacts of changes in source conditions on temperature estimates along AIM events at EDC and EDML hence strengthening the conclusion of Jouzel et al. (2003). Still, being aware of the aforementioned limitations, we only use the $\delta^{18}O$ variations over AIM events as qualitative indications for the amplitude of the temperature changes in Antarctica, with a correspondence between $\delta^{18}O$ and temperature ranging between 0.4 and 0.8‰/°C.

The $\delta^{18}O$ of the TALDICE ice core has been measured with a depth resolution of 1 m (bag sample). The new TALDICE data presented in this study are covering a depth interval ranging from 850 m to 1199 m (20–50 ky BP). The mean temporal resolution of this dataset is 91 years. TALDICE $\delta^{18}O$ bag samples were measured in Italy (Trieste and Parma Universities) and France (LSCE) according to well-established techniques (Epstein et al., 1953; Vaughn et al., 1998; Stenni et al., 2011). δD was measured in Italy using the H_2/water equilibration method with an automatic HDO device coupled to a mass spectrometer. The $\delta^{18}O$ data provided here result from at least duplicate measurements of 346 samples. The analytical precision of $\delta^{18}O$ and δD measurements is ±0.05‰ and ±0.7‰, respectively.

3.3. Deuterium excess and $ssNa^{+}$ data

3.3.1. The deuterium excess proxy

The deuterium excess, d-excess = $\delta D - 8 \times \delta^{18}O$ (Dansgaard, 1964), is a second-order isotopic parameter, containing information about conditions prevailing in the source regions of Antarctic precipitation. The d-excess is imprinted by the initial evaporation conditions (Merlivat and Jouzel, 1979) but is also influenced by (1) the equilibrium fractionation associated with air mass cooling (slight dependency on temperature of the fractionation ratio of δD and $\delta^{18}O$ and therefore on the apparent meteoric water line) and (2) by kinetic fractionation taking place during ice crystal formation (Jouzel and Merlivat, 1984). Ice core d-excess therefore provides integrated information on past changes in moisture sources and/or air mass trajectories.

At each phase of the hydrological cycle (evaporation, condensation…), equilibrium and kinetic fractionations affect the isotopic composition of water in the vapour and condensed phase. The two types of fractionations do not affect similarly $\delta^{18}O$ and δD so that these two parameters do not exhibit exactly the same signal. While δD and $\delta^{18}O$ variations in polar snow indicate at first order changes in the local temperature, d-excess contains information about the temperature and relative humidity of the oceanic source providing Antarctic precipitation (Vimeux et al., 1999; Stenni et al., 2001). It is also slightly influenced by the final condensation temperature and isotopic composition of the ocean. From simple isotopic models tuned for EDC (Masson-Delmotte et al., 2004) or EDML (Stenni et al., 2010), the theoretical slope of the relationship between d-excess and site temperature is ~−0.5‰/°C. The uncertainty on this slope is difficult to estimate, as it depends on uncertainties in isotopic model parameterizations, as well as on the range of temperatures between evaporation and condensation. For inland sites such as Dome Fuji or Vostok, slopes up to −1.3‰/°C have recently been suggested (Uemura et al., 2012). While $\delta^{18}O$ or d-excess are also affected by changes in oceanic isotopic composition, this effect can be neglected on time scales of AIM events. We conclude that TALDICE d-excess variations over AIM events should

mostly be sensitive to evaporation conditions at the oceanic moisture source.

The TALDICE d-excess data have been calculated on 346 samples between 20 and 50 ky BP from the raw $\delta^{18}O$ and δD signals with an overall precision of $\pm 0.8‰$.

3.3.2. The $ssNa^+$ proxy

Sea-salt concentrations in Antarctic aerosols were originally interpreted in terms of changes in storminess, which was supposed to be the main driver of both aerosol production and inland transport (Petit et al., 1981; Delmas, 1992). Then, the formation of sea-salt aerosol by atmospheric uplift of frost flowers was proposed as a significant source of sea spray for coastal areas of Antarctica (Rankin et al., 2002; Wolff et al., 2003). Frost flowers provide a large effective surface area and a reservoir of sea-salt ions in the liquid phase with ion concentrations up to three times higher than seawater (Perovich and Richter-Menge, 1994; Rankin et al., 2002). The sea-salt concentration in the seawater trapped in the sea-ice pockets is due to the sea-salt exclusion during the freezing processes leading to the formation of new sea ice. This enriched source could explain the higher $ssNa^+$ concentrations measured in the aerosol and in the snow deposition in winter and during cold periods. Changes in source intensity and typology and/or variations in transport pathways and efficiency can also affect past variations in $ssNa^+$ deposition. Limitations of this proxy have been raised recently. First, it is not clear yet whether the flux of sea salt to the ice sheet represents primarily an indicator of ice production or sea ice extent (Wolff et al., 2010). Second, the sensitivity of sea-salt flux to sea ice extent is probably non-linear and seems to show a weaker response during period of large ice sheet extends (Fischer et al., 2007; Röthlisberger et al., 2010). However, keeping this in mind, $ssNa^+$ records from Antarctic ice cores still provide unique information on past sea-ice extent and persistence around Antarctica (Wolff et al., 2006; Fischer et al., 2007; Röthlisberger et al., 2008).

In the following, we cautiously use new $ssNa^+$ data from TALDICE to qualitatively discuss sea ice extent variations in the Ross Sea area in comparison with information inferred from existing $ssNa^+$ records from the EPICA drilling sites.

320 samples of the TALDICE ice core were measured for $ssNa^+$ concentrations between 848.5 and 1188.5 m of depth, corresponding to the 20–50 ky BP range. $SsNa^+$concentrations are translated into fluxes by multiplying with the accumulation rate deduced from the inverse method for dating discussed below (Lemieux-Dudon et al., 2009; Buiron et al., 2011).

3.4. Ice cores age scales

In order to precisely investigate the timing of the climate signals in the different sites and to compare them to the model findings, it is necessary to rely on consistent and accurate age scales.

Between 20 and 50 ky BP, the TALDICE-1 age scale (Buiron et al., 2011) mainly relies on (1) the synchronization of the TALDICE methane profile with the Greenland composite record (Blunier et al., 2007) on the absolute GICC05 age scale from Greenland ice cores (Svensson et al., 2008), and (2) the use of a new inverse method for ice core dating (Lemieux-Dudon et al., 2009). The TALDICE-1 uncertainty reaches 1500 years between 20 and 25 ky BP and typically lies between 450 and 650 yr in the period between 25 and 50 ky BP (see Appendix for more details). The chronological uncertainty thus remains smaller than the duration of the AIM events themselves, enabling a pluri-centennial time scale study of the timing and duration of each event.

For the EDC and EDML ice cores, we used the chronologies calculated by Lemieux-Dudon et al. (2010) with the same inverse method. Therefore TALDICE, EDML, and EDC time scales are all based on a synchronisation with the Greenland GICC05 absolute chronology (Svensson et al., 2008). The relative uncertainties associated with each age scale are low enough during the last 50 ky (±100–800 yr at EDML, ±70–800 yr) at EDC (Lemieux-Dudon et al., 2010) to allow for investigation of the timing, shape and duration of rapid climatic events between the three sites.

For the other ice cores, unfortunately, such precise synchronisation is not available and lies beyond the scope of this manuscript. We used their latest official time scales: the Byrd time scale built by Blunier and Brook (2001), the Vostok age scale improved by Lemieux-Dudon et al. (2010), the Siple Dome time scale built by Brook et al. (2005), the Dome F time scale built by Kawamura et al. (2007), and the Taylor Dome chronology improved by Grootes et al. (2001) from the initial one built by Steig et al. (1998). The time resolution of isotopic data for each ice core is summarized in Table 1. We therefore focus our analysis on the three synchronised records, and compare the main findings with the remaining five ice cores on their own chronology in Table 2. We are aware that the chronology is an issue in such a comparison so that the comparison given in Table 2 should be considered with caution.

4. Results

4.1. $\delta^{18}O$ records from TALDICE and EPICA ice cores

The TALDICE $\delta^{18}O$ record during the MIS 3 period is shown in the upper part of Fig. 5, compared to its EDC, EDML, and NorthGRIP counterparts on a common timescale. This enables to study within the same chronological framework the expression of the millennial time scale climatic variability in three different sectors of Antarctica. The signal depicts a millennial-scale variability pattern very similar to the one observed in the EPICA ice cores, with slow $\delta^{18}O$ increases during the Greenland stadials and $\delta^{18}O$ decreases during the Greenland interstadials. With the resolution of our measurements on the TALDICE ice core, 10 over 12 AIM events can be distinguished between 20 and 50 ky BP. Within the chronological uncertainties and limitations associated with the sampling resolution, the sequence of events from TALDICE appears as a direct bipolar response with respect to the Greenlandic NorthGRIP record. The TALDICE signal shares the EDC triangular AIM event shapes previously described, in opposition to the EDML squared shapes. This is particularly visible on the AIM events 8 and 12. The fact that the AIM event shapes are similar between EDC and TALDICE suggests that both sites share similar oceanic influences, probably from the Indian Ocean (EPICA Community Members, 2006; Stenni et al., 2010, 2011).

In order to better quantify spatial differences, we summarize the AIM events 8 and 12 warming amplitudes and rate of changes for all available ice cores around Antarctica in Table 2 (also see Fig. S3 in the Appendix). We focus on those particular two events for two reasons. First, they are associated with a clear Heinrich event as evidenced from marine cores hence making the comparison with modelling experiments driven by a freshwater flux more direct. Second, these climatic events are the longest and present the largest warming amplitudes observed between 20 and 50 ky BP. This enables to clearly depict the signal shape. For EDC, EDML and TALDICE ice cores we estimated the duration of the warming phase for each event by calculating the first derivative of the isotopic record (see Appendix for details). The relative associated uncertainty when comparing the three ice cores is estimated to be ±300 yr. For the remaining ice cores, our estimate is only indicative because their chronologies are less accurate and in particular not consistent with the one of EDC, EDML and TALDICE.

The EDML warming rate appears twice higher than in TALDICE and EDC ice cores, and seems to take place on a 40% shorter

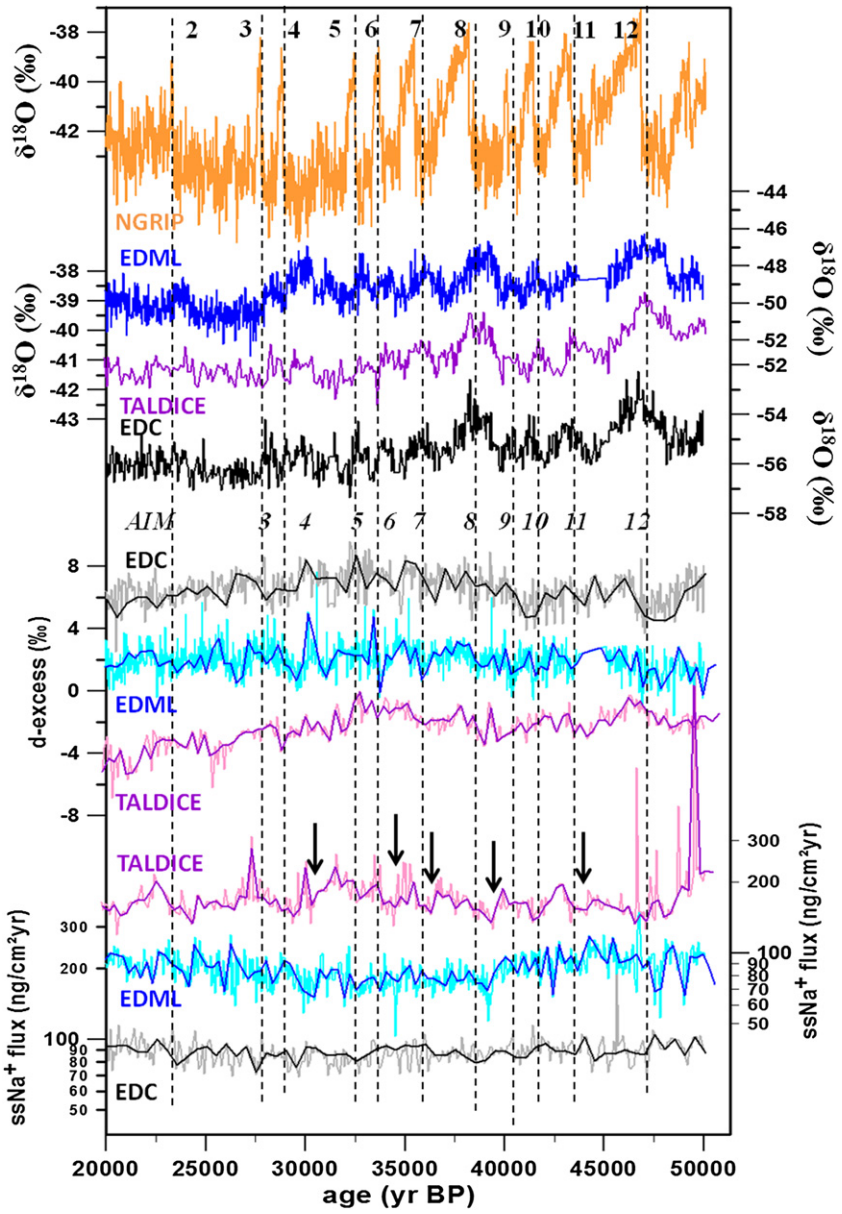

Fig. 5. $\delta^{18}O$, $ssNa^{+}$ flux and deuterium excess signals recorded at TALDICE (purple lines), EDML (blue line) and EDC (black line) between 20 and 50 ky. SsNa and d-excess data are re-sampled to 500 yr at EDC and at 300 yr at EDML and TALDICE (width lines). AIM events are numbered. The NGRIP isotopic signal is represented with an orange line and DO events are numbered at the top and pointed by black dashed lines. Black arrows underline $ssNa^{+}$ decreases at EDML and TALDICE at the beginning of AIM events. (For interpretation of the references to colour in this figure legend, the reader is referred to the web version of this article.)

duration (910 yr vs 1600 yr for both EDC and TALDICE). In the Atlantic sector, the Dome F warming also is significantly faster, which strengthens the hypothesis of a more rapid response of the Atlantic sector to an AMOC weakening. Age scale uncertainties do not allow assessing further the discrepancies of the different signals.

4.2. d-excess and $ssNa^{+}$ records at TALDICE, EDML and EDC drilling sites

Sea-salt sodium and deuterium excess records are compared to the water isotopic profiles for EDML, EDC and TALDICE (Fig. 5).

4.2.1. Deuterium excess

The mean MIS3 d-excess (~−2‰) is significantly lower at TALDICE than at EDML (~2‰) and EDC (~6‰) between 30 and 50 ky BP (Fig. 5). This gradient is also currently observed and likely reflects a stronger contribution of high latitude moisture sources to TALDICE, consistent with present-day back-trajectory analyses and modelling (Delaygue et al., 2000; Reijmer et al., 2002; Sodemann and Stohl, 2009; Scarchilli et al., 2011; Masson-Delmotte et al., 2011).

Millennial-scale features are visible in the TALDICE d-excess signal between 25 and 50 ky BP. For some AIM events (AIM event 8 and less clearly for the AIM events 7 and 11), an antiphase pattern can be distinguished between $\delta^{18}O$ and d-excess, the d-excess starting to increase when $\delta^{18}O$ has reached a maximum (Fig. 6). This feature is actually more marked in the EDC ice core (Stenni et al., 2010), and cannot be explained by the small impact of limited site temperature changes on deuterium excess (see Section 3.3.2). Variations of d-excess during AIM events are thus related to moisture source changes. Because paleoceanographic

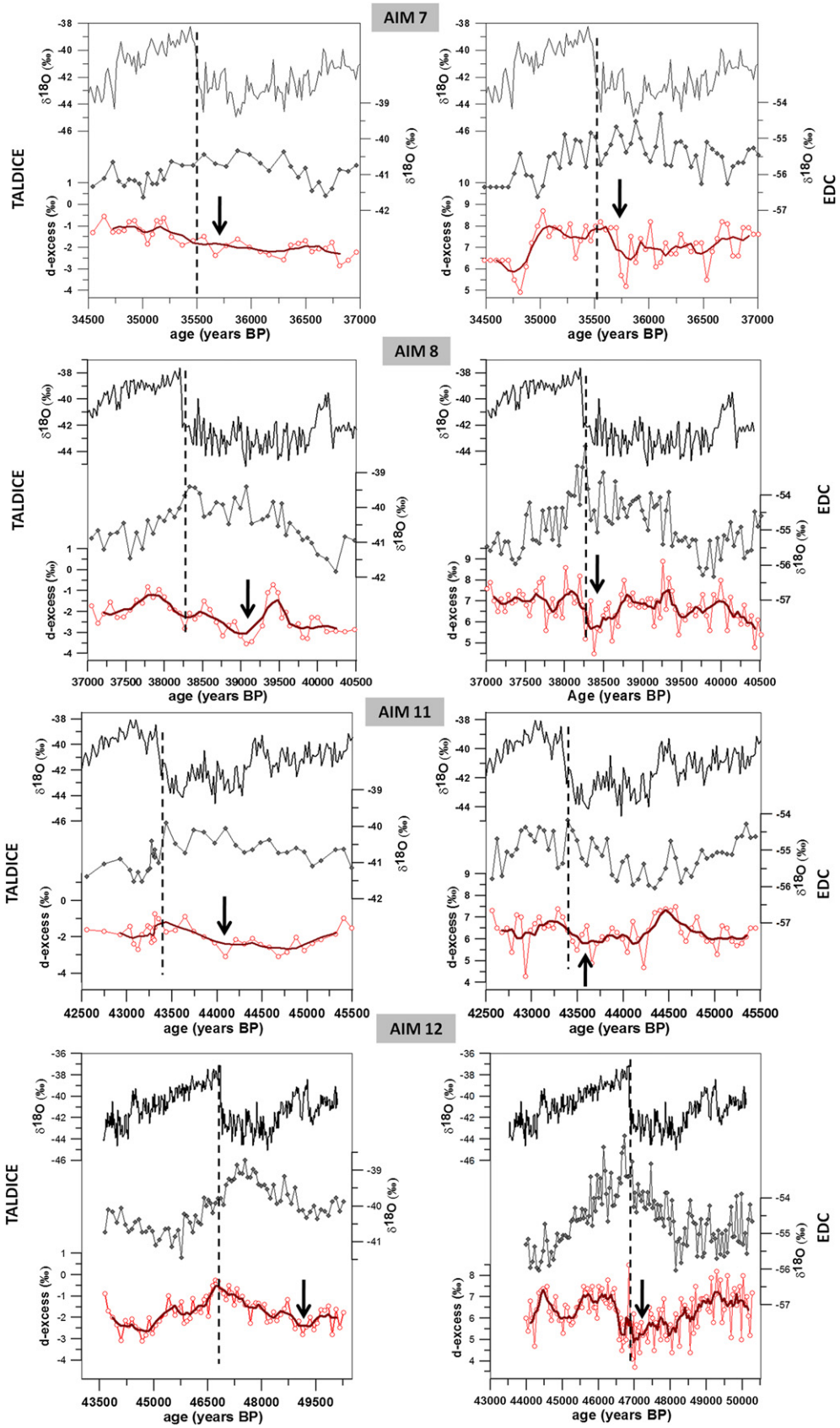

Fig. 6. Comparison between TALDICE and EDC isotopic records over four AIM events. For AIM events 7, 8, 11 and 12: representation of the TALDICE (on the left) and EDC (on the right) $\delta^{18}O$ (black diamonds) and d-excess (red circles) records, plotted on their own time scales, and compared to the NorthGRIP water isotopic record (full black line) represented on the GICC05 chronology. A running average line on five points has been added to the d-excess profile (brown line). In each case the dashed line underlines the DO transition and an arrow points the lowest d-excess value preceding the DO transition. (For interpretation of the references to colour in this figure legend, the reader is referred to the web version of this article.)

reconstructions of SST in the southern Indian Ocean follow the general pattern of Antarctic temperature (Mazaud et al., 2000), changes in SST at a given area cannot explain the d-excess signal. We therefore interpret the anti-correlation between d-excess and local temperature as a southward shift of the location of oceanic source regions during the warm phases of AIM events. Such reorganizations of oceanic source regions around Antarctica are also observed over terminations (Masson-Delmotte et al., 2010) and could be linked to latitudinal shifts of the westerlies (Lamy et al., 2007; Schmidt et al., 2007) and/or to sea ice extent variations. The same scenario is probably at play for AIM events at EDC and EDML (Stenni et al., 2010).

We also note peculiarities of the TALDICE (and to a lesser extent EDML) d-excess signal, especially over AIM event 8, and to a lesser extent in the AIM events 7, 11, and 12 (Fig. 6): (1) the d-excess increase is more gradual at TALDICE than at EDC; (2) the minimum of d-excess at TALDICE appears earlier than the AIM event $\delta^{18}O$ maximum while the two events are in phase at EDC. This last point suggests that the reorganization of the atmospheric circulation occurs earlier in the moisture source regions of TALDICE (high latitudes) than in the moisture source regions of EDC (lower latitudes) (Ding et al., 2011). The earlier d-excess changes recorded at the TALDICE coastal site support fast changes in moisture source areas preceding the bipolar temperature seesaw impact in Antarctic temperature.

4.2.2. Comparison of the $ssNa^+$ records

Higher sea-salt sodium fluxes (ranging between 200 and 600 ng/cm^2 yr) are observed at TALDICE compared to EDML (between 100 and 400 ng/cm^2 yr) and especially EDC (around 100 ng/cm^2 yr). This probably reflects the reduced distance of TALDICE to the open ocean with respect to both EPICA sites (Table 1).

The first comparison of $ssNa^+$ records between TALDICE, EDML and EDC shows that $ssNa^+$ variations are stronger in the coastal sites than on the EDC site. Then, as already underlined by Fischer et al. (2007), no clear correlation can be distinguished between the water isotopes increase during AIM events and the variation of the $ssNa^+$ signal at EDC. However the TALDICE $ssNa^+$ signal shares some EDML features over the AIM events 11, 8, 7, 6 and 4, showing similar rapid decreases at the onset of each AIM event (arrows in Fig. 5) followed by gradual recoveries to higher values. At EDML, this structure was interpreted as an abrupt reduction of sea ice in response to the southern warming (Fischer et al., 2007). If the same mechanism for sea ice extent is at play for TALDICE and EDML, two potential implications can be proposed from the observed TALDICE $ssNa^+$ rapid variations:

(1) Small increases of SAT temperature at the onsets of AIM events have huge impact on sea ice extent over the Ross Sea/Indian region (amplifying the SAT changes).
(2) If sea ice extent reacts to sea surface temperature (SST) evolution, SST changes over the Ross Sea and over the Indian sector of the SO are more abrupt than the temperature evolution recorded in TALDICE $\delta^{18}O$.

5. Discussion

5.1. Comparison between simulations and ice core data during AIM events

The comparison of $\delta^{18}O$ evolutions over the different ice cores has revealed the same AIM event patterns at TALDICE and EDC, notably through similar durations of warming phases (Table 2). This suggests (1) a predominant contribution of Indian moisture source at Talos Dome under glacial conditions, which is supported by modern back-trajectories studies (Scarchilli et al., 2011; Masson-Delmotte et al., 2011); (2) and/or that the Southern Pacific Ocean warms slowly and in phase with the Indian Ocean. Finally, $\delta^{18}O$ records from West Antarctica (Siple Dome and Byrd) reveal very well depicted AIM events of triangular shapes with amplitude for the $\delta^{18}O$ increases comparable to what is observed in the Indian sector (Table 2).

By contrast, much more rapid temperature rises are identified in the ice cores located in the Atlantic sector, EDML and to a lesser extent Dome F, where the warming duration is twice as short as in the Indian sector (Table 2). While the Indian/Pacific Ocean sector warming persists during the whole Greenland stadial period until the next DO event starts in the North Atlantic, the total warming of the Atlantic sector of the SO is reached during the first half of the stadial.

Although the model-data comparison is limited by the short duration of the simulations (less than 1000 years) compared to the usual length of the Greenland stadial and by the idealized design of the freshwater hosing scenario, some patterns are observed both in ice core data and model simulations. The contrast between the different AIM event warming durations in the Atlantic and Indian sectors are very consistent with our simulations where a rapid warming anomaly appears first in the Atlantic sector, before it gradually propagates to the Indian sector. Strong Atlantic temperature fluctuations are also consistent with the high sea ice sensitivity to different boundary conditions observed in the Weddell Sea area from marine data (Crosta et al., 2004; Stuut et al., 2004; Gersonde et al., 2005).

Both model and ice core data results thus support the two proposed drivers of the SO response to a reduced AMOC: (1) a bipolar seesaw of ocean heat transport, which generates some delay for building up warming around the Antarctic continent (200–350 yr in the simulation); (2) deviations from this warming induced by the bipolar seesaw, due to a fast atmospheric-surface ocean teleconnection originating from the tropics. In the IPSL-CM4 model, this teleconnection is related to SST changes in the tropical Atlantic, which is the ocean basin over which there are the largest changes due to the freshwater hosing. In other models, a similar mechanism has also been observed but originating from the tropical East Pacific (Timmermann et al., 2010).

While a quantitative model-data comparison remains difficult because it would need a more realistic scenario in terms of boundary conditions and hosing as well as longer simulations, we note that the magnitude of the strongest isotopic changes (Table 2) suggests a minimum temperature anomaly of 1.8–6.4 °C (using the modern spatial slope, which may underestimate magnitudes, see Section 3.2). This is a hint that the IPSL-CM4 (producing temperature changes < 1.2 °C) as well as other models simulating a response of the same order for a hosing under glacial boundary conditions (Merkel et al., 2010; Otto-Bliesner and Brady, 2010) may underestimate the magnitude of AIM events. Further quantitative investigations would require explicit isotopic modelling within the climate model.

Despite the general qualitative consistency between the IPSL-CM4 and the isotopic records, several disagreements are also observed. The very clear and high amplitude triangular shapes of AIM events observed in ice cores located in West Antarctica are not supporting the simulated cooling in the Siple Dome and Byrd regions (Fig. 1b, Table 2). Moreover, temperature reconstructions from marine sediment cores near southern Chile show a general agreement with the AIM events features in West Antarctica (Lamy et al., 2004; Kaiser et al., 2005). The simulated West Antarctic pattern and cooling over the East Pacific sector of the SO therefore appears unrealistic.

Several reasons can be invoked to explain this mismatch. Firstly, the dipole simulated between East and West Antarctica is centred

on coastal areas (Figs. 1 and 2). By contrast, the simulated Indian sector warming affects a larger spatial extent with significant imprints observed over the whole East Antarctic plateau. It is thus possible that the AIM event pattern observed in ice core records over a large part of Antarctica is controlled by climate changes occurring in the Indian sector and does not resolve the regional peri-Antarctic SO variability. Furthermore, the radiative impact of millennial time scale fluctuations of atmospheric greenhouse gas concentrations accompanying stadials/interstadials (CH_4) and AIM events (CO_2) (Timmermann et al., 2010) are expected to drive coherent temperature changes in Antarctica, and amplify AIM event amplitudes. These were not taken into account in our idealized experimental design. In order to assess the consistency of temperature changes around Antarctica, and the validity of the IPSL simulated coastal pattern, a complete circum-Antarctic network of high-resolution marine records is needed for MIS3. While some marine records already exists that suggest coherent and simultaneous temperature changes in Antarctica and SO (Caniupán et al., 2011), a detail comparison of marine and ice core records from the three ocean basins placed on a coherent and climate independent chronology is still lacking but is beyond the scope of this work.

As already stated, the set-up of the numerical experiments analysed in Section 2 is also extremely simple. A continuous 0.1 Sv freshwater flux is imposed in the North Atlantic, resulting in an AMOC collapse, which is rather slow since it occurs in a few hundred years. It would be interesting to investigate the signals resulting from the bipolar seesaw and tropical-extratropical teleconnections in response to faster or slower AMOC collapses. Furthermore, the LGM boundary conditions used here are not exactly those of MIS 3 (Van Meerbeeck et al., 2009). Swingedouw et al. (2009) have shown that a cooling occurs in the southeastern Pacific as a response to freshwater hosing, for the LGM and future climates, but not for the Holocene and preindustrial climates. Thus, a sensitivity study with respect to the associated mean changes in orbital context, ice volume and CO_2 would be interesting. Moreover, these studies show that fast mechanisms can have an impact in modulating a basic bipolar seesaw response, but much is left to investigate about the timing and spatial impact of these fast responses.

5.2. Coastal vs. inland sites behaviour during abrupt temperature changes

We now explore the observational and model evidences to test the hypothesis of a stronger imprint of regional changes in coastal versus more inland ice cores.

The millennial time scale variations observed in the d-excess signals recorded in EDML, EDC and TALDICE ice cores suggest that AMOC fluctuations are accompanied by a reorganization of the atmospheric circulation and/or a change in the location of the oceanic evaporative regions feeding the precipitation at the three sites.

At EDC a classical signal is observed where d-excess begins to increase simultaneously with the beginning of the Greenland interstadial (Masson-Delmotte et al., 2010; Stenni et al., 2010), i.e. when local temperature in Antarctica starts to decrease. This situation is consistent with previous investigations that have shown that abrupt shutdown (recovery) of the AMOC strength during Heinrich (DO) events leads to a southward (northward) displacement of the ITCZ, which modifies the ascendance branch of the atmospheric circulation and excites Rossby waves. As a consequence the stationary waves in the high latitudes are modified through this tropical–extratropical teleconnection (Deser et al., 2004) and induces stronger (weaker) westerlies winds in the Southern Hemisphere. Such reorganization implies a modulation of the relative contributions of low versus high latitude moisture. We therefore suggest that the d-excess increase observed at EDC at the onset of the Greenland interstadial reflects the northward shift of moisture sources induced by the weakening of the SH westerly winds linked with AMOC recovery (Schmidt et al., 2007; Stenni et al., 2010).

The d-excess increase observed at EDML and TALDICE is more gradual and leads the peak AIM event signal. This suggests that for more peripheral sites, the d-excess variability is probably strongly driven by regional SST variations and moisture source changes, possibly also impacted by local sea ice extent. This suggestion is supported by the coincident variability observed in the TALDICE and EDML $ssNa^+$ records.

As a perspective, sensitivity tests should be performed with atmospheric general circulation models equipped with the modelling of stable isotopes and water tagging, in response to the ocean surface patterns provided by the coupled model outputs (e.g. Langen and Vinther, 2008; Masson-Delmotte et al., 2011). Such simulations would be particularly useful to perform more quantitative model-data comparisons, to assess the realism of the magnitude of the simulated changes, and hopefully to understand the local versus remote moisture source signals in the ice core records. Recent high-resolution simulations have indeed demonstrated the ability of isotopic atmospheric models to resolve modern regional features (Werner et al., 2011). Moreover multimodel comparisons would allow assessing the robustness of the IPSL-CM4 results.

6. Conclusions and perspectives

In this manuscript, we have first presented results from simulations performed by a global coupled atmosphere-ocean model (IPSL-CM4) under glacial conditions and compared them to the results of other models. Our aim was to investigate the SO and Antarctica responses to freshwater fluxes assumed to drive the millennial time scale variability occurring between 20 and 50 ky BP. Two (out of three) simulations performed under glacial conditions highlight strong differences in the regional response of the different geographic sectors of the SO (Atlantic, Pacific, and Indian), as already suggested by previous studies performed with other global coupled models under modern boundary conditions. The question then arises of the possibility of a zonally asymmetric response to a perturbation in the Atlantic Meridional Overturning Circulation. Model results as well as studies of the recent evolution of the Antarctic climate (Ding et al., 2011) show that this climatic signature would likely consist of two distinct mechanisms: the gradual bipolar seesaw effect and faster atmospheric teleconnections linking the tropics (in the case of the IPSL-CM4 model, the tropical Atlantic) and specific regions of the SO (in our case the southern Pacific area). We have confronted the model results with climatic data extracted from ice core records. We have thus presented a review of MIS3 AIM event expression from all the available Antarctica ice core water isotopic records and complemented this review through new data from the TALDICE ice core. Our data suggest that the TALDICE site is mostly under the Indian Ocean influence. To better depict the phasing between the different regional expressions, we have performed detailed comparisons of the three ice cores that have a new common chronology (EDML, EDC and TALDICE). Although all sites share a clear bipolar seesaw signal, the compilation of water isotopic records is consistent with the simulated temperature change in the Atlantic sector reacting immediately to the freshwater flux, and a slower response in the Indian sector. A distinct difference of the climate evolution of the Indo-Pacific and Atlantic sectors is also observed during millennial events of the last deglaciation (Stenni et al., 2010, 2011).

In addition to the water isotopic records, we have presented new $ssNa^+$ fluxes and d-excess records over the TALDICE ice core between 20 and 50 ky BP and compared them with their counterparts in the EPICA (EDC and EDML) ice cores. The general anti-correlation observed between d-excess and $\delta^{18}O$ at the three sites suggests a major reorganization of the hydrological cycle (changes in the moisture source location) potentially induced by shifts in the ITCZ and modification of the SH westerlies intensity or position, in response to an AMOC shutdown. Coastal sea ice may also significantly influence such reorganization as suggested by the early d-excess increase observed at TALDICE and EDML, during the stadial phase, coinciding with significant $ssNa^+$ decreases at the beginning of each AIM event at both sites.

While AIM event shapes and amplitudes measured in ice cores are similar in the Indian and East Pacific sectors, the model produces a rather flat signal in West Antarctica. New climatic simulations runs under various conditions would be needed to investigate the origin of this model-data mismatch. Simulations including water stable isotopes and water tagging would allow a more quantitative comparison.

In order to go beyond the comparison of the three sites and also look at the phasing between sea ice modification, moisture source location and Antarctic temperature at the western side of Antarctica, d-excess and $ssNa^+$ data from West Antarctica ice cores are strongly needed. In these perspectives, the data from the new WAIS ice core (Fegyveresi et al., 2011) will be especially useful. Besides, getting isotopic data from an ice core drilled in a coastal site facing the Pacific Sector of Antarctica could provide a better spatial and temporal quantification of the dipole pattern, simulated by the model.

Finally, the robustness of the circum-Antarctic patterns requires comparing the ice core records with other paleoclimatic archives such as marine sedimentary cores drilled in the different ocean basins to characterize SST, salinity and sea ice variations in the SO during the MIS3 period.

Acknowledgements

We thank the logistic and drilling TALDICE team. The Talos Dome Ice Core Project (TALDICE), a joint European programme led by Italy, is funded by national contributions from Italy, France, Germany, Switzerland and the United Kingdom. The main logistical support was provided by Programma Nazionale di Ricerche in Antartide (PNRA) at Talos Dome. This is TALDICE publication no 24.

Appendix B. Supplementary data

Supplementary data related to this article can be found online at http://dx.doi.org/10.1016/j.quascirev.2012.05.023.

References

Alkama, R., Kageyama, M., Ramstein, G., Marti, O., Ribstein, P., Swingedouw, D., 2007. Impact of a realistic river routing in coupled ocean–atmosphere simulations of the Last Glacial Maximum climate. Climate Dynamics 30, 855–869.

Alvarez-Solas, J., Ramstein, G., 2011. On the triggering mechanism of Heinrich events. Proceedings of the National Academy of Sciences 108 (50), E1359–E1360.

Barker, S., Diz, P., Vautravers, M.J., Pike, J., Knorr, G., Hall, I.R., Broecker, W.S., 2009. Interhemispheric Atlantic seesaw response during the last deglaciation. Nature 457, 1097–1102.

Berger, A.L., 1978. Long term variations of daily insolation and quaternary climatic changes. Journal of the Atmospheric Sciences 35 (12), 2362–2367.

Blunier, T., Chappellaz, J., Schwander, J., Dallenbach, A., Stauffer, B., Stocker, T.F., Raynaud, D., Jouzel, J., Clausen, H.B., Hammer, C.U., Johnsen, S.J., 1998. Asynchrony of Antarctic and Greenland climate change during the last glacial period. Nature 394, 739–743.

Blunier, T., Brook, E.J., 2001. Timing of millennial-scale climate change in Antarctica and Greenland during the last glacial period. Science 291, 109–112.

Blunier, T., Spahni, R., Barnola, J.M., Chappellaz, J., Loulergue, L., Schwander, J., 2007. Synchronization of ice core records via atmospheric gases. Climate of the Past 3, 325–330.

Braconnot, P., Otto-Bliesner, B., Harrison, S., Joussaume, S., Peterchmitt, J.-Y., Abe-Ouchi, A., Crucifix, M., Driesschaert, E., Fichefet, T., Hewitt, C.D., kageyama, M., Kitoh, A., Laîné, A., Loutre, M.-F., Marti, O., Merkel, U., Ramstein, G., Valdes, P., Weber, S.L., Yu, Y., Zhao, Y., 2007. Results of PMIP2 coupled simulations of the mid-Holocene and Last Glacial Maximum – part 1: experiments and large-scale features. Climate of the Past 3, 261–277.

Broccoli, A.J., Dahl, K.A., Stouffer, R.J., 2006. Response of the ITCZ to northern Hemisphere cooling. Geophysical Research Letters 33, L01702. http://dx.doi.org/10.1029/2005GL024546.

Broecker, W., 1998. Paleocean circulation during the last deglaciation: a bipolar seesaw? Paleoceanography 13, 119–121.

Brook, E.J., White, J.W., Schilla, A.S., Bender, M.L., Barnett, B., Severinghaus, J.P., Taylor, K.C., Alley, R.B., Steig, E.J., 2005. Timing of millennial-scale climate change at Siple Dome, West Antarctica, during the last glacial period. Quaternary Science Reviews 24, 1333–1343.

Buiron, D., Chappellaz, J., Stenni, B., Frezzotti, M., Baumgartner, M., Capron, E., Landais, A., Lemieux-Dudon, B., Masson-Delmotte, V., Montagnat, M., Parrenin, F., Schilt, A., 2011. TALDICE-1 age scale of the Talos Dome deep ice core, East Antarctica. Climate of the Past 7, 1–16.

Caniupán, M., Lamy, F., Lange, C.B., Kaiser, J., Arz, H., Kilian, R., Baeza Urrea, O., Aracena, C., Hebbeln, D., Kissel, C., Laj, C., Mollenhauer, G., Tiedemann, R., 2011. Millennial-scale sea surface temperature and Patagonian ice sheet changes off southernmost Chile (53°S) over the past ~60 kyr. Paleoceanography 26 (3221). http://dx.doi.org/10.1029/2010PA002049.

Capron, E., Landais, A., Lemieux-Dudon, B., Schilt, A., Masson-Delmotte, V., Buiron, D., Chappellaz, J., Dahl-Jensen, D., Johnsen, S.J., Leuenberger, M., Loulergue, L., Oerter, H., 2010. Synchronising EDML and NorthGRIP ice cores using $\delta^{18}O$ of atmospheric oxygen ($\delta^{18}O_{atm}$) and CH_4 measurements over MIS 5 (80–123 kyr). Quaternary Science Reviews 29, 222–234.

Clement, A.C., Peterson, L.C., 2008. Mechanisms of abrupt climate change of the last glacial period. Reviews of Geophysics 46, RG4002. http://dx.doi.org/10.1029/2006RG000204.

Crosta, X., Sturm, A., Armand, L., Pichon, J.-J., 2004. Late Quaternary sea-ice history in the Indian sector of the Southern Ocean as recorded by diatom assemblages. Marine Micropaleontology 50, 209–223.

Crowley, T.J., 1992. North Atlantic deep water cools the Southern Hemisphere. Paleoceanography 7, 489–497.

Dahl, K.A., Broccoli, A.J., Stouffer, R.J., 2005. Assessing the role of North Atlantic freshwater forcing in millennial scale climate variability: a tropical Atlantic perspective. Climate Dynamics 24, 325–346.

Dällenbach, A., Blunier, T., Flückiger, J., Stauffer, B., Chappellaz, J., Raynaud, D., 2000. Changes in the atmospheric CH_4 gradient between Greenland and Antarctica during the Last Glacial and the transition to the Holocene. Geophysical Research Letters 27, 1005–1008.

Dansgaard, W., 1964. Stable isotopes in precipitation. Tellus 16, 436–468.

Dansgaard, W., Johnsen, S.J., Clausen, H.B., Dahl-Jensen, D., Gundestrup, N.S., Hammer, C.U., Hvidberg, C.S., Steffensen, J.P., Sveinbjörnsdottir, A.E., Jouzel, J., Bond, G., 1993. Evidence for general instability of past climate from a 250-ky ice-core record. Nature 364, 218–220.

Delaygue, G., Edouard, B., Schmidt, G., Labeyrie, L., Vidal, L., Genthon, C., Jouzel, J., 2000. Relations entre surface océanique et composition isotopique des précipitations antarctiques: simulation pour différents climats. PhD thesis, Universite de Droite, d'Economie et des Sciences d'Aix-Marseille.

Delmas, R.J., 1992. Environmental information from ice cores. Reviews of Geophysics 30, 1–21.

Deser, C., Phillips, A.S., Hurrell, J.W., 2004. Pacific interdecadal climate variability: linkages between the tropics and the North Pacific during Boreal Winter since 1900. Journal of Climate 17, 3109–3124.

Ding, Q., Steig, E.J., Battisti, D.S., Kuttel, M., 2011. Winter warming in West Antarctica caused by central tropical Pacific warming. Nature Geoscience 4, 398–403.

Elliot, M., Labeyrie, L., Duplessy, J.-C., 2002. Changes in North Atlantic deep-water formation associated with the Dansgaard–Oeschger temperature oscillations (60-10 ky). Quaternary Science Reviews 21, 1153–1165.

EPICA Community Members, 2004. Eight glacial cycles from an Antarctic ice core. Nature 429, 623–628.

EPICA Community Members, 2006. One-to-one coupling of glacial climate variability in Greenland and Antarctica. Nature 444, 195–198.

Epstein, S., Buchsbaum, R., Lowenstam, L., Urey, H., 1953. Carbonate-water isotopic temperature scale. Geological Society of America Bulletin 62, 417–425.

Fegyveresi, J.M., Alley, R.B., Spencer, M., Fitzpatrick, J.J., Steig, E.J., White, J.W.C., Mcconnell, J., Taylor, K.C., 2011. Late-Holocene climate evolution at the WAIS Divide site, WestAntarctica: bubble number-density estimates. Journal of Glaciology 57, 629–638.

Fischer, H., Fundel, F., Ruth, U., Twarloh, B., Wegner, A., Udisti, R., Becagli, S., Castellano, E., Morganti, A., Severi, M., Wolff, E., Littot, G., Röthlisberger, R., Mulvaney, R., Hutterli, M., Kaufmann, P., Federer, U., Lambert, F., Bigler, M., Hansson, M., Jonsell, U., De Angelis, M., Boutron, C., Siggaard-Andersen, M.-L., Steffensen, J.P., Barbante, C., Gaspari, V., Gabrielli, P., Wagenbach, D., 2007. Reconstruction of millenial changes in dust emission, transport and regional sea-ice coverage using the deep EPICA ice cores from the Atlantic and Indian Ocean sector of Antarctica. Earth and Planetary Science Letters 260, 340–354.

Flückiger, J., Dällenbach, A., Blunier, T., Stauffer, B., Stocker, T.F., Raynaud, D., Barnola, J.-M., 1999. Variations in atmospheric N_2O concentration during abrupt climatic changes. Science 285, 227–230.
Frezzotti, M., Bitelli, G., de Michelis, P., Deponti, A., Forieri, A., Gandolfi, S., Maggi, V., Mancini, F., Remy, F., Tabacco, I.E., 2004. Geophysical survey at Talos Dome, East Antarctica: the search for a new deep-drilling site. Annals of Glaciology 39, 423–432.
Frezzotti, M., Urbini, S., Proposito, M., Scarchilli, C., Gandolfi, S., 2007. Spatial and temporal variability of surface mass balance near Talos Dome, East Antarctica. Journal of Geophysical Research 112, F02032. http://dx.doi.org/10.1029/2006JF000638.
Gersonde, R., Crosta, X., Abelmann, A., Armand, L., 2005. Sea-surface temperature and sea-ice distribution of the Southern Ocean at the EPILOG Last Glacial Maximum—a circum-Antarctic view based on siliceous microfossil records. Quaternary Science Reviews 24, 869–896.
Grootes, P.M., Steig, E.J., Stuiver, M., Waddington, E.D., Morse, D.L., Nadeau, M.-J., 2001. The Taylor Dome antarctic ^{18}O record and globally synchronous changes in climate. Quaternary Research 56, 289–298.
Heinrich, H., 1988. Origin and consequences of cyclic ice rafting in the Northeast Atlantic Ocean during the past 130,000 years. Quaternary Research 29, 142–152.
Jouzel, J., Merlivat, L., 1984. Deuterium and oxygen 18 in precipitation: modeling of the isotopic effects during snow formation. Journal of Geophysical Research 89, 11749–11757.
Jouzel, J., Vimeux, F., Caillon, N., Delaygue, G., Hoffmann, G., Masson-Delmotte, V., Parrenin, F., 2003. Magnitude of the isotope-temperature scaling for interpretation of central Antarctic ice cores. Journal of Geophysical Research 108, 1029–1046.
Jouzel, J., Masson-Delmotte, V., Cattani, O., Dreyfus, G., Falourd, S., Hoffmann, G., Minster, B., Nouet, J., Barnola, J.M., Chappellaz, J., Fischer, H., Gallet, J.C., Johnsen, S., Leuenberger, M., Loulergue, L., Luethi, D., Oerter, H., Parrenin, F., Raisbeck, G., Raynaud, D., Schilt, A., Schwander, J., Selmo, E., Souchez, R., Spahni, R., Stauffer, B., Steffensen, J.P., Stenni, B., Stocker, T.F., Tison, J.L., Werner, M., Wolff, E.W., 2007. Orbital and millennial antarctic climate variability over the past 800,000 Years. Science 317, 793–796.
Kageyama, M., Mignot, J., Swingedouw, D., Marzin, C., Alkama, R., Marti, O., 2009. Glacial climate sensitivity to different states of the Atlantic meridional overturning circulation: results from the IPSL model. Climate of the Past Discussions 5, 1055–1107.
Kageyama, M., Paul, A., Roche, D.M., Van Meerbeeck, C.J., 2010. Modelling glacial climatic millennial-scale variability related to changes in the Atlantic meridional overturning circulation: a review. Quaternary Science Reviews 29, 2931–2956.
Kaiser, J., Lamy, F., Hebbeln, D., 2005. A 70-kyr sea surface temperature record off southern Chile (Ocean Drilling Program Site 1233). Paleoceanography 20 (4009). http://dx.doi.org/10.1029/2005PA001146.
Kawamura, K., Parrenin, F., Lisiecki, L., Uemura, R., Vimeux, F., Severinghaus, J.P., Hutterli, M.A., Nakazawa, T., Aoki, S., Jouzel, J., Raymo, M.E., Matsumoto, K., Nakata, H., Motoyama, H., Fujita, S., Goto-Azuma, K., Fujii, Y., Watanabe, O., 2007. Northern Hemisphere forcing of climatic cycles in Antarctica over the past 360,000 years. Nature 448, 912–916.
Krebs, U., Timmermann, A., 2007. Fast advective recovery of the Atlantic meridional overturning circulation after a Heinrich event. Paleoceanography 22.
Krinner, G., Werner, M., 2003. Impact of precipitation seasonality changes on isotopic signals in polar ice cores: a multi-model analysis. Earth and Planetary Science Letters 216, 525–538.
Lamy, F., Kaiser, J., Ninnemann, U., Hebbeln, D., Arz, H.W., Stoner, J., 2004. Antarctic timing of surface water changes off Chile and Patagonian ice sheet response. Science 304, 1959–1962.
Lamy, F., Kaiser, J., Arz, H.W., Hebbeln, D., Ninnemann, U., Timm, O., Timmermann, A., Toggweiler, J.R., 2007. Modulation of the bipolar seesaw in the southeast Pacific during termination 1. Earth and Planetary Science Letters 259, 400–413.
Landais, A., Caillon, N., Goujon, C., Grachev, A.M., Barnola, J.M., Chappellaz, J., Jouzel, J., Masson-Delmotte, V., Leuenberger, M., 2004. Quantification of rapid temperature change during DO event 12 and phasing with methane inferred from air isotopic measurements. Earth and Planetary Science Letters 225, 221–232.
Lang, C., Leuenberger, M., Schwander, J., Johnsen, S., 1999. 16 °C rapid temperature variation in central Greenland 70,000 years ago. Science 286, 934–937.
Langen, P.L., Vinther, B.M., 2008. Response in atmospheric circulation and sources of Greenland precipitation to glacial boundary conditions. Climate Dynamics 32, 1035–1054.
Lemieux-Dudon, B., Parrenin, F., Blayo, E., 2009. A probabilistic method to construct a common and optimal chronology for an ice core. In: Hondoh (Ed.). Hokkaido University Collection of Scholarly and Academic Papers.
Lemieux-Dudon, B., Blayo, E., Petit, J.R., Waelbroeck, C., Svensson, A., Ritz, C., Barnola, J., Narcisi, B.M., Parrenin, F., 2010. Consistent dating for Antarctic and Greenland ice cores. Quaternary Science Reviews 29, 8–20.
Lorius, C., Merlivat, L., Jouzel, J., Pourchet, M., 1979. A 30,000-yr isotope climatic record from Antarctic ice. Nature 280, 644–648.
Manabe, S., Stouffer, R.J., 1988. Two stable equilibria of a coupled ocean-atmosphere model. Journal of Climate 1, 841–866.
Marti, O., Braconnot, P., Dufresne, J.-L., Bellier, J., Benshila, R., Bony, S., Brockmann, P., Cadule, P., Caubel, A., Codron, F., Noblet, N., Denvil, S., Fairhead, L., Fichefet, T., Foujols, M.-A., Friedlingstein, P., Goosse, H., Grandpeix, J.-Y., Guilyardi, E., Hourdin, F., Idelkadi, A., kageyama, M., Krinner, G., Lévy, C., Madec, G., Mignot, J., Musat, I., Swingedouw, D., Talandier, C., 2010. Key features of the IPSL ocean atmosphere model and its sensitivity to atmospheric resolution. Climate Dynamics 34, 1–26.
Masson-Delmotte, V., Stenni, B., Jouzel, J., 2004. Common millennial-scale variability of Antarctic and Southern Ocean temperatures during the past 5000 years reconstructed from the EPICA Dome C ice core. The Holocene 14, 145–151.
Masson-Delmotte, V., Hou, S., Ekaykin, A., Jouzel, J., Aristarain, A., Bernardo, R.T., Bromwich, D., Cattani, O., Delmotte, M., Falourd, S., Frezzotti, M., Gallée, H., Genoni, L., Isaksson, E., Landais, A., Helsen, M.M., Hoffmann, G., Lopez, J., Morgan, V., Motoyama, H., Noone, D., Oerter, H., Petit, J.R., Royer, A., Uemura, R., Schmidt, G.A., Schlosser, E., Simões, J.C., Steig, E.J., Stenni, B., Stievenard, M., van den Broeke, M.R., van de Wal, R.S.W., van de Berg, W.J., Vimeux, F., White, J.W.C., 2008. A review of Antarctic surface snow isotopic composition: observations, atmospheric circulation, and isotopic modeling. Journal of Climate 21, 3359–3387.
Masson-Delmotte, V., Stenni, B., Blunier, T., Cattani, O., Chappellaz, J., Cheng, H., Dreyfus, G., Edwards, R.L., Falourd, S., Govin, A., kawamura, K., Johnsen, S.J., Jouzel, J., Landais, A., Lemieux-Dudon, B., Lourantou, A., Marshall, G., Minster, B., Mudelsee, M., Pol, K., Röthlisberger, R., Selmo, E., Waelbroeck, C., 2010. Abrupt change of Antarctic moisture origin at the end of termination II. Proceedings of the National Academy of Sciences 107, 12091–12094.
Masson-Delmotte, V., Buiron, D., Ekaykin, A., Frezzotti, M., Gallée, H., Jouzel, J., Krinner, G., Landais, A., Motoyama, H., Oerter, H., Pol, K., Pollard, D., Ritz, C., Schlosser, E., Sime, L.C., Sodemann, H., Stenni, B., Uemura, R., Vimeux, F., 2011. A comparison of the present and last interglacial periods in six Antarctic ice cores. Climate of the Past 7, 397–423.
Mazaud, A., Vimeux, F., Jouzel, J., 2000. Short fluctuations in Antarctic isotope records: a link with cold events in the North Atlantic? Earth and Planetary Science Letters 177, 219–225.
McManus, J.F., Francois, R., Gherardi, J.M., Keigwin, L.D., Brown-Leger, S., 2004. Collapse and rapid resumption of Atlantic meridional circulation linked to deglacial climate changes. Nature 428, 834–837.
Merkel, U., Prange, M., Schulz, M., 2010. ENSO variability and teleconnections during glacial climates. Quaternary Science Reviews 29, 86–100.
Merlivat, L., Jouzel, J., 1979. Global climatic interpretation of the deuterium-oxygen 18 relationship for precipitation. Journal of Geophysical Research 84, 5029–5033.
Monnin, E., Indermühle, A., Dällenbach, A., Flückiger, J., Stauffer, B., Stocker, T.F., Raynaud, D., Barnola, J.-M., 2001. Atmospheric CO_2 concentrations over the Last Glacial Termination. Science 291, 112–114.
Oerter, H., Graf, W., Meyer, H., Wilhelms, F., 2004. The EPICA ice core from Dronning Maud Land: first results from stable-isotope measurements. Annals of Glaciology 39, 307–312.
Otto-Bliesner, B.L., Brady, E.C., 2010. The sensitivity of the climate response to the magnitude and location of freshwater forcing: last glacial maximum experiments. Quaternary Science Reviews 29, 56–73.
Peltier, W.R., 2004. Global glacial isostasy and the surface of the ice-age earth: the ICE-5G (VM2) model and GRACE. Annual Review of Earth and Planetary Sciences 32, 111–149.
Perovich, D.K., Richter-Menge, J.A., 1994. Surface characteristics of lead ice. Journal of Geophysical Research 99, 16,341–16,350.
Petit, J.-R., Briat, M., Royer, A., 1981. Ice age aerosol content from East Antarctic ice core samples and past wind strength. Nature 293, 391–394.
Petit, J.R., Jouzel, J., Raynaud, D., Barkov, N.I., Barnola, J., Basile, I., Bender, M., Chappellaz, J., Davis, M., Delaygue, G., Delmotte, M., Kotlyakov, V.M., Legrand, M., Lipenkov, V.Y., Lorius, C., PEpin, L., Ritz, C., Saltzman, E., Stievenard, M., 1999. Climate and atmospheric history of the past 420,000 years from the Vostok ice core, Antarctica. Nature 399, 429–436.
Rankin, A.M., Wolff, E.W., Martin, S., 2002. Frost flowers: Implications for tropospheric chemistry and ice core interpretation. Journal of Geophysical Research 107, 15.
Reijmer, C.H., Van den Broeke, M.R., Scheele, M.P., 2002. Air parcel trajectories and snowfall related to five deep drilling locations in Antarctica based on the ERA-15 dataset. Journal of Climate 15, 1957–1968.
Roche, D.M., Wiersma, A.P., Renssen, H., 2010. A systematic study of the impact of freshwater pulses with respect to different geographical locations. Climate Dynamics 34, 997–1013.
Röthlisberger, R., Mudelsee, M., Bigler, M., de Angelis, M., Fischer, H., Hansson, M., Lambert, F., Masson-Delmotte, V., Sime, L., Udisti, R., Wolff, E.W., 2008. The Southern hemisphere at glacial terminations: insights from the Dome C ice core. Climate of the Past 4, 345–356.
Röthlisberger, R., Crosta, X., Abram, N.J., Armand, L., Wolff, E.W., 2010. Potential and limitiations of marine and ice core sea ice proxies: an example from the Indian Ocean sector. Quaternary Science Reviews 29, 296–302.
Scarchilli, C., Frezzotti, M., Ruti, P.M., 2011. Snow precipitation at four ice core sites in East Antarctica: provenance, seasonality and blocking factors. Climate Dynamics 37, 2107–2125.
Schmidt, G.A., LeGrande, A.N., Hoffmann, G., 2007. Water isotope expressions of intrinsic and forced variability in a coupled ocean-atmosphere model. Journal of Geophysical Research 112, D10103. http://dx.doi.org/10.1029/2006JD007781.
Severinghaus, J.P., Sowers, T., Brook, E.J., Alley, R.B., Bender, M.L., 1998. Timing of abrupt climate change at the end of the Younger Dryas interval from thermally fractionated gases in polar ice. Nature 391, 141–146.

Sime, L.C., Wolff, E.W., Oliver, K.I.C., Tindall, J.C., 2009. Evidence for warmer interglacials in East Antarctic ice cores. Nature 462, 342–345.
Sodemann, H., Stohl, A., 2009. Asymmetries in the moisture origin of Antarctic precipitation. Geophysical Research Letters 36, L22803. http://dx.doi.org/10.1029/2009GL040242.
Steig, E.J., Brook, E., White, J., Sucher, C., 1998. Synchronous climate changes in Antarctica and the north Atlantic. Science 282, 92–95.
Stenni, B., Masson-Delmotte, V., Johnsen, S., Jouzel, J., Longinelli, A., Monnin, E., Röthlisberger, R., Selmo, E., 2001. An oceanic cold reversal during the last deglaciation. Science 293, 2074–2077.
Stenni, B., Proposito, M., Gragnani, R., Flora, O., Jouzel, J., Falourd, S., Frezzotti, M., 2002. Eight centuries of volcanic signal and climate change at Talos Dome (East Antarctica). Journal of Geophysical Research 107. http://dx.doi.org/10.1029/2000JD000317.
Stenni, B., Masson-Delmotte, V., Selmo, E., Oerter, H., Meyer, H., Röthlisberger, R., Jouzel, J., Cattani, O., Falourd, S., Fischer, H., 2010. The deuterium excess records of EPICA Dome C and Dronning Maud land ice cores (East Antarctica). Quaternary Science Reviews 29, 146–159.
Stenni, B., Buiron, D., Frezzotti, M., Albani, S., Barbante, C., Bard, E., Barnola, J.M., Baroni, M., Baumgartner, M., Bonazza, M., Capron, E., Castellano, E., Chappellaz, J., Delmonte, B., Falourd, S., Genoni, L., Iacumin, P., Jouzel, J., Kipfstuhl, S., Landais, A., Lemieux-Dudon, B., Maggi, V., Masson-Delmotte, V., Mazzola, C., Minster, B., Montagnat, M., Mulvaney, R., Narcisi, B., Oerter, H., Parrenin, F., Petit, J.R., Ritz, C., Scarchilli, C., Schilt, A., Schupbach, S., Schwander, J., Selmo, E., Severi, M., Stocker, T.F., Udisti, R., 2011. Expression of the bipolar seesaw in Antarctic climate records during the last deglaciation. Nature Geoscience 4, 46–49.
Stocker, T.F., 1998. Climate change: the seesaw effect. Science 282, 61–62.
Stocker, T.F., Johnsen, S., 2003. A minimum thermodynamic model for the bipolar seesaw. Paleoceanography 18, 1087. http://dx.doi.org/10.1029/2003PA000920.
Stouffer, R.J., Yin, J., Gregory, J.M., Dixon, K.W., Spelman, M.J., Hurlin, W., Weaver, A.J., Eby, M., Flato, G.M., Hasumi, H., Hu, A., Jungclaus, J.H., kamenkovich, I.V., Levermann, A., Montoya, M., Murakami, S., Nawrath, S., Oka, A., Peltier, W.R., Robitaille, D.Y., Sokolov, A., Vettoretti, G., Weber, S.L., 2006. Investigating the causes of the response of the thermohaline circulation to past and future climate changes. Journal of Climate 19, 1365–1387.
Stuut, J.B., Crosta, X., Van Der Borg, K., Schneider, R., 2004. Relationship between Antarctic sea-ice and southwest African climate during the late Quaternary. Geology 32, 909.
Svensson, A., Andersen, K.K., Bigler, M., Clausen, H.B., Dahl-Jensen, D., Davies, S.M., Johnsen, S.J., Muscheler, R., Parrenin, F., Rasmussen, S.O., 2008. A 60 000 year Greenland stratigraphic ice core chronology. Climate of the Past 4, 47–57.
Swingedouw, D., Mignot, J., Braconnot, P., Mosquet, E., Kageyama, M., Alkama, R., 2009. Impact of freshwater release in the North Atlantic under different climate conditions in an OAGCM. Journal of Climate 22, 6377–6403.
Timmermann, A., Menviel, L., Okumura, Y., Schilla, A., Merkel, U., Timm, O., Hu, A., Otto-Bliesner, B., Schulz, M., 2010. Towards a quantitative understanding of millennial-scale Antarctic warming events. Quaternary Science Reviews 29, 74–85.
Uemura, R., Masson-Delmotte, V., Jouzel, J., Landais, A., Motoyama, H., Stenni, B., 2012. Ranges of moisture-source temperature estimated from Antarctic ice cores stable isotope records over glacial-interglacial cycles. Climate of the Past 8, 1109–1125.
Van Meerbeeck, C.J., Renssen, H., Roche, D.M., 2009. How did Marine Isotope Stage 3 and Last Glacial Maximum climates differ?—Perspectives from equilibrium simulations. Climate of the Past 5, 33–51.
Van Ommen, T., Morgan, V., 1997. Calibrating the ice core paleothermometer using seasonality. Journal of Geophysical Research 102, 9351–9357.
Vaughn, B.H., White, J.W.C., Delmotte, M., Trolier, M., Cattani, O., Stievenard, M., 1998. An automated system for hydrogen isotope analysis of water. Chemical Geology 152, 309–319.
Vidal, L., Labeyrie, L., Cortijo, E., Arnold, M., Duplessy, J.C., Michel, E., Becqué, S., van Weering, T.C.E., 1997. Evidence for changes in the North Atlantic deep water linked to meltwater surges during the Heinrich events. Earth and Planetary Science Letters 146, 13–27.
Vimeux, F., Masson, V., Jouzel, J., Stievenard, M., Petit, J.R., 1999. Glacial-interglacial changes in ocean surface conditions in the Southern Hemisphere. Nature 398, 410–413.
Watanabe, O., Jouzel, J., Johnsen, S., Parrenin, F., Shoji, H., Yoshida, N., 2003. Homogeneous climate variability across East Antarctica over the past three glacial cycles. Nature 422, 509–512.
Werner, M., Langebroek, P.M., Carlsen, T., Herold, M., Lohmann, G., 2011. Stable water isotopes in the ECHAM5 general circulation model: toward high-resolution isotope modeling on a global scale. Journal of Geophysical Research 116, D15109. http://dx.doi.org/10.1029/2011JD015681.
Wolff, E.W., Rankin, A., Rothlisberger, R., 2003. An ice core indicator of Antarctic sea-ice production? Geophysical Research Letters 30 (22), 2158. http://dx.doi.org/10.1029/2003GL018454.
Wolff, E.W., Fischer, H., Fundel, F., Ruth, U., Twarloh, B., Littot, G.C., Mulvaney, R., Röthlisberger, R., de Angelis, M., Boutron, C.F., Hansson, M., Jonsell, U., Hutterli, M.A., Lambert, F., kaufmann, P., Stauffer, B., Stocker, T.F., Steffensen, J.P., Bigler, M., Siggaard-Andersen, M.L., Udisti, R., Becagli, S., Castellano, E., Severi, M., Wagenbach, D., Barbante, C., Gabrielli, P., Gaspari, V., 2006. Southern Ocean sea-ice extent, productivity and iron flux over the past eight glacial cycles. Nature 440, 491–496.
Wolff, E.W., Barbante, C., Becagli, S., Bigler, M., Boutron, C.F., Castellano, E., de Angelis, M., Federer, U., Fischer, H., Fundel, F., Hansson, M., Hutterli, M., Jonsell, U., Karlin, T., Kaufmann, P., Lambert, F., Littot, G.C., Mulvaney, R., Röthlisberger, R., Ruth, U., Severi, M., Siggaard-Andersen, M.L., Sime, L.C., Steffensen, J.P., Stocker, T.F., Traversi, R., Twarloh, B., Udisti, R., Wagenbach, D., Wegner, A., 2010. Changes in environment over the last 800,000 years from chemical analysis of the EPICA Dome C ice core. Quaternary Science Reviews 29, 285–295.